Letter

Spectroscopic Evidence of Size-Dependent Buffering of Interfacial pH by Cation Hydrolysis during CO Electroreduction

Onagie Ayemoba, and Angel Cuesta

Just Accepted

Spectroscopic Evidence of Size-Dependent Buffering of Interfacial pH by Cation Hydrolysis during CO_2 Electroreduction

Onagie Ayemoba and Angel Cuesta*

Department of Chemistry, School of Natural and Computing Sciences, University of Aberdeen, AB24 3UE Aberdeen, Scotland, UK

Supporting Information Placeholder

ABSTRACT: The nature of the electrolyte cation is known to affect the Faradaic efficiency and selectivity of CO_2 electroreduction. Singh et al. (*J. Am. Chem. Soc.* **2016**, *138*, 13006–13012) recently attributed this effect to the buffering ability of cation hydrolysis at the electrical double layer. According to them, the pK_a of hydrolysis decreases close to the cathode due to the polarization of the solvation water molecules sandwiched between the cation's positive charge and the negative charge on the electrode surface. We have tested this hypothesis experimentally, by probing the pH at the gold-electrolyte interface *in situ* using ATR-SEIRAS. The ratio between the integrated intensity of the CO_2 and HCO_3^- bands, which has to be inversely proportional to the concentration of H^+, provided a means to determining the pH change at the electrode-electrolyte interface *in-situ* during the electroreduction of CO_2. Our results confirm that the magnitude of the pH increase at the interface follows the trend $Li^+ > Na^+ > K^+ > Cs^+$, adding strong experimental support to Singh's et al.'s hypothesis. We show, however, that the pH buffering effect was overestimated by Singh et al., their overestimation being larger the larger the cation. Moreover, our results show that the activity trend of the alkali-metal cations can be inverted in the presence of impurities that alter the buffering effect of the electrolyte, although the electrolyte with maximum activity is always that for which the increase of the interfacial pH is smaller.

Keywords: CO_2RR; ATR-SEIRAS; cation effects; cation hydrolysis; interfacial pH.

Much effort has been devoted in recent years to the development of efficient systems for the electroreduction of CO_2 to fuels or other valuable chemicals.[1] Among the many factors (surface composition,[1,2] structure[3–6] and morphology,[7,8] temperature,[9] pressure,[10] CO_2 flow rate,[11] etc.) affecting the activity and selectivity of a given electrode towards the CO_2 reduction reaction (CO_2RR), pH has been shown to play a critical role. The optimal pH for the CO_2RR has been found to lie around 7, but at the cathode-electrolyte interface protons are depleted due to the CO_2RR and the hydrogen evolution reaction (HER, the main competing reaction decreasing CO_2RR's Faradaic efficiency), and the pH can easily rise 2 units or more above that in the bulk, even when using buffer solutions (the most usual of which are CO_2-saturated $MHCO_3$ solutions for obvious reasons, with M an alkaline metal).

It has been known since Hori's pioneering work that the nature of the cation in CO_2-saturated $MHCO_3$ buffer solutions affects the efficiency and selectivity of the CO_2RR.[12] Although known since the 1930's,[13] the effect of cations on the kinetics of electrochemical reactions has recently received renewed attention due to unexpected effects on fuel-cell relevant reactions.[14] Frumkin's explanation of the effect of cations on the reduction of an electrochemically active species is based on the existence of a difference between the electrostatic potential at the outer Helmholtz plane (ϕ_{OHP}) and in the bulk of the electrolyte (ϕ_s).[15] If the electroactive species is charged, this will affect the energy required to bring it from the bulk to the OHP, where electron transfer happens, and through it, its concentration at the OHP and the reaction rate. If the electroactive species is neutral (like CO_2), an effect might still exist, as the potential drop felt by it ($\phi_m - \phi_{OHP}$, the driving force for electron transfer, with ϕ_m the electrode's Galvani potential) will be less than the potential difference between the electrode surface and the bulk of the solution ($\phi_m - \phi_s$). This model can explain changes in the reaction rate observed when the concentration of a given cation increases but, in the absence of specific adsorption, it cannot explain differences between cations at the same concentration, because the effect of the cation radius on ϕ_{OHP} is known to be negligible.[16] Markovic's qualitative explanation of the effect of cations[14] cannot explain their effect on the CO_2RR either, because it relies on attractive non-covalent interactions between the cations and specifically adsorbed anions, absent at the very negative potentials at which the CO_2RR takes place. The quantitative model recently developed by our group[17–19] can be considered to integrate Frumkin's and Markovic's approaches, as it takes into account both electrostatic interactions of the cations with specifically adsorbed anions and the difference between ϕ_s and ϕ_{OHP}. Therefore, it cannot account for their effect on the CO_2RR either.

Singh et al.[20] recently suggested an alternative hypothesis, according to which hydrolysis of the cation's solvation layer would have a buffering effect on the interfacial pH. According to them, the pK_a of hydrolysis decreases close to the cathode due to the polarization of the solvation water molecules sandwiched between the cation's positive charge and the negative charge on the electrode surface. The resulting buffering ability increases with increasing cation size and decreasing hydration number ($Cs^+ > K^+ > Na^+ > Li^+$). Keeping the pH at the interface closer to that in the bulk increases the concentration of CO_2 available for reduction at the interface, increasing the catalytic activity and the Faradaic efficiency of the process. We have tested this hypothesis experimentally, by probing the pH at the gold-electrolyte interface *in situ* using surface-enhanced infrared absorption spectroscopy in the attenuated total reflection mode (ATR-SEIRAS). Our results confirm that the magnitude of the pH increase at the interface during the electrocatalytic reduction of CO_2 follows the trend $Li^+ > Na^+ > K^+ > Cs^+$, although the decrease of the pK_a of cation

hydrolysis at the interface, and, hence, the resulting buffering effect, was overestimated by Singh et al., especially in the case of the largest cations.

The concentrations of CO_2 and HCO_3^- at the interface must be in equilibrium with each other, and will be determined by the local pH:

$$\frac{a_{CO_2}}{a_{HCO_3^-}} = \frac{a_{H^+}}{K_a} \qquad \text{Eq. 1}$$

where K_a is the first dissociation constant of CO_2, and a_{CO_2}, $a_{HCO_3^-}$, a_{H^+} are the activities of CO_2, HCO_3^- and H^+, respectively, which can be substituted in a first approximation by their corresponding concentrations. Both CO_2 and HCO_3^- have C–O stretching vibrational modes with strong absorptions in the infrared. The integrated absorbance of the corresponding bands must follow Beer-Lambert Law, and will be proportional to the concentration of the absorbing species. Accordingly:

$$\log \frac{I_{CO_2}}{I_{HCO_3^-}} = A - \text{pH} \qquad \text{Eq. 2}$$

where I_{CO_2} and $I_{HCO_3^-}$ are the integrated intensities of the CO_2 and HCO_3^- bands, respectively, and $A = pK_a + \log \frac{\varepsilon_{CO_2} l_{CO_2}}{\varepsilon_{HCO_3^-} l_{HCO_3^-}}$, with ε_{CO_2} and $\varepsilon_{HCO_3^-}$ the absorption coefficients of CO_2 and HCO_3^-, respectively, and l_{CO_2} and $l_{HCO_3^-}$ the length of electrolyte probed at the frequencies corresponding to CO_2 and HCO_3^-, respectively. *I.e.*, the logarithm of the ratio between the integrated absorbance of the CO_2 and HCO_3^- bands will decrease or increase in one unit if the pH increases or decreases, respectively, in one unit. We would like to note that the equilibrium between CO_2 and HCO_3^- is relatively slow. For this reason, the experiments reported below were performed during a slow linear sweep voltammogram (LSV) of 1 mV s^{-1}, and the spectra recorded were the result of the addition of 120 interferograms. We believe that, under these experimental conditions, it is reasonable to assume that the concentrations of CO_2 and HCO_3^- at the interface reach equilibrium before the system experiences a significant perturbation of the potential (and, hence, of the pH), and that the spectra obtained correspond to that equilibrium situation

In ATR-SEIRAS, the infrared beam is totally reflected at the interface between an IR-transparent window (in our case Si) and the electrolyte. A thin (ca. 30 to 50 nm) metal film (in our case Au) is deposited on the Si surface in contact with the electrolyte, and is used as the working electrode of an electrochemical cell (for more experimental details, please see the Supporting Information). Under these conditions, the IR beam does not cross the interface into the electrolyte, and only a narrow region of the solution just above the electrode (that corresponding to the penetration depth of the evanescent wave minus the thickness of the metal film, roughly between 200 and 500 nm in the 4000–1000 cm^{-1} frequency range) is probed. In principle, this would make ATR-SEIRAS an ideal technique to probe the composition (in this specific case, the pH) of the interfacial region However, unless the target species has a strong IR absorption and/or is present at high concentrations, bands corresponding to species in solution are usually weak in ATR-SEIRAS, and typically weaker than those of adsorbed species, because the SEIRA effect only extends over ca. 10 nm from the surface.[21] This is illustrated in Fig. S1, which shows the spectrum of an as-prepared Au film on Si in CO_2-saturated 0.1 M $LiHCO_3$, obtained using the spectrum of the same film in pure water as background. Although the bands corresponding to the COO asymmetric stretching of HCO_3^- ($\nu_{COO, asym}$) and, particularly, of CO_2 (ν_{co_2}), can be clearly seen, they are too weak, preventing the determination of the ratio between their integrated intensities with a good enough signal-to-noise ratio, as

required for the determination of the interfacial pH. We found, however, that submitting the film to three cycles at 50 mV s^{-1} between 0.7 and 1.3 V in 0.1 M HCl provokes a significant increase of the intensity of the HCO_3^- and CO_2 bands, as also shown in Fig. S1, without significantly affecting the optical appearance or the conductivity of the film. We attribute this effect to a slight decrease of the film thickness (which allows accessing a region where the electric field of the evanescent wave is more intense) and to an increase of the film roughness. It is also likely that the latter allows trapping some electrolyte in small voids within the film, in which the CO_2 molecules and HCO_3^- ions could fall within the reach of the SEIRA effect. This allows us to determine $\frac{I_{CO_2}}{I_{HCO_3^-}}$ with a good signal-to-noise ratio, and to employ ATR-SEIRAS to probe *in situ* the pH of the interface during the CO2RR. This is similar to a recent work in which the pH- and potential-dependent ratio between the integrated intensities of the carbonyl and carboxylate bands in ATR-SEIRA spectra of self-assembled monolayers (SAMs) of 11-mercaptoundecanoic acid (MUA) was used to determine the pK_a of MUA in the SAM.[22]

The proximity between $\nu_{COO, asym}$ and the H-O-H bending mode of water (δ_{HOH}) also needs to be taken into account. As shown recently by Yamakata et al. using CO-covered Pt electrodes,[23–25] ATR-SEIRAS can be used to obtain the vibrational spectrum of the hydration layer of the cations of the supporting electrolyte at the electrode-electrolyte interface. Fig. S2 shows potential-dependent ATR-SEIRA spectra between 0 and -1.0 V *vs.* Ag/AgCl(KCl$_{sat}$), obtained with an Au film in 0.1 M NH_4ClO_4 using the spectrum at 0 V as background. Three bands are observed to increase with increasing negative potential, at 3500 cm^{-1}, 1630 cm^{-1}, and 1450 cm^{-1}, corresponding to the O-H stretching mode of water ν_{OH}, δ_{HOH}, and the $-(NH_3)$ (δ_s) mode of NH_4^+, respectively. These three bands grow in parallel, which is evidence that they correspond to the same species, namely, the hydrated NH_4^+ ion. The consequence of this is illustrated in Fig. S3, in which the current and the ratio between the integrated intensities of the CO_2 band and of the band in the $1630 - 1650$ cm^{-1} region in a CO_2-saturated 0.1 M $NaHCO_3$ solution have been plotted as a function of the electrode potential. The ratio between I_{CO_2} and $I_{HCO_3^-}$ starts decreasing more or less linearly at potentials clearly more positive than the current onset, at which only double-layer charging occurs, and at which no pH increase is possible. This is a clear indication that the increase in the intensity of the band at $1630 - 1650$ cm^{-1} is due to the accumulation of Na^+ ions at the interface when the negative charge density on the electrode surface increases. This problem can be easily solved, though, by using D_2O as the solvent, for which the water bending mode shifts down into the region around 1230 cm^{-1}.
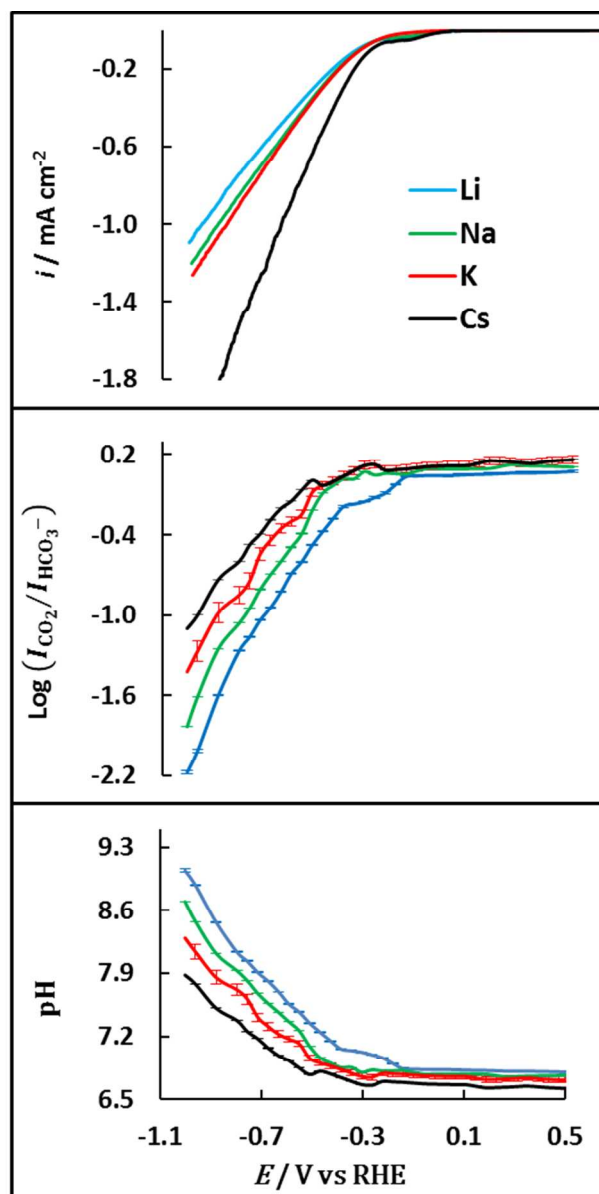
Figure 1. LSVs at 1 mV s^{-1} (top panel) of a thin-film Au electrode on Si in CO$_2$-saturated 0.05 M M$_2$CO$_3$ solutions (M = Li (blue), Na (green), K (red), Cs (black)) in D$_2$O, potential dependence of the $I_{CO_2}/I_{HCO_3^-}$ ratio (mid panel) as obtained from simultaneously recorded ATR-SEIRA spectra, and potential dependence of the interfacial pH (bottom panel).

Fig. S4 shows selected ATR-SEIRA spectra of the Au-electrolyte interface recorded at increasingly negative potentials during a linear potential sweep at 1 mV s^{-1} between 0.4 and -1.0 V in CO$_2$-saturated 0.05 M M$_2$CO$_3$ (M = Li, Na, K or Cs). Fig. 1 shows the corresponding LSVs, the potential dependence of $\log\frac{I_{CO_2}}{I_{HCO_3^-}}$, and the resulting pH-potential curves (for details regarding the conversion of $\log\frac{I_{CO_2}}{I_{HCO_3^-}}$ into pH units see the Supporting Information).

The current density at potentials more negative than the onset of the reaction increases with increasing atomic radius (Fig. 1, top panel), in agreement with the trend observed by Singh et al.,[20] and others before them.[12,26,27] As the potential is made more negative and the current increases, both I_{CO_2} and $I_{HCO_3^-}$ decrease due to the CO2RR (Fig. S4), but the ratio between them does not remain constant (Fig. 1, middle panel). The relative amount of HCO$_3^-$

increases in all cases at increasing negative potentials due to the increase of the interfacial pH. However, the pH increase is not the same in all cases, and follows the trend Li$^+$ > Na$^+$ > K$^+$ > Cs$^+$ (Fig. 1, bottom panel). These differences in the interfacial pH can only be due to different buffering capacities of the supporting electrolyte, and, since the electrolytes used only differ in the cation, our results provide strong experimental support to Singh's et al.'s model.
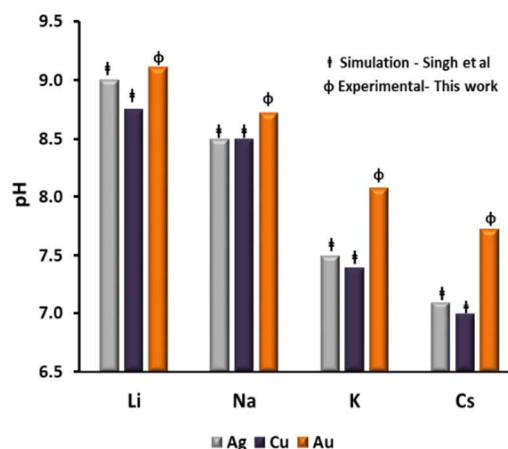

Figure 2. Steady-state pH at the metal-electrolyte interface during the electroreduction of CO$_2$ at -1 V vs. RHE in CO$_2$-saturated 0.05 M M$_2$CO$_3$ solutions (M = Li, Na, K, Cs). pH values for Ag and Cu correspond to those resulting from Singh's et al.'s calculations,[20] while in the case of Au they correspond to our experimental determination using ATR-SEIRAS.

Singh et al.[20] calculated the pK_a for the hydrolysis of the alkaline metal cations using Equation 3:

$$pK_a = -A\left(\frac{z^2}{r_{M\text{-}O}} + 2\pi\sigma z r_{H\text{-}el}\left(\sqrt{1 + \frac{r_{M\text{-}O}^2}{r_{H\text{-}el}^2}} - 1\right)\right) + B \qquad \text{Eq. 3}$$

where $-A\frac{z^2}{r_{M\text{-}O}} + B$ accounts for the pK_a in the bulk,[28,29] and

$-A2\pi\sigma z r_{H\text{-}el}\left(\sqrt{1 + \frac{r_{M\text{-}O}^2}{r_{H\text{-}el}^2}} - 1\right)$ accounts for the change in pK_a

due to polarization of the water molecules in the solvation shell sandwiched between the positive charge of the cation and the negative charge on the electrode surface.[20] A and B are constants with values 620.32 pm and 17.154, respectively,[20] z is the effective charge on the cation, $r_{M\text{-}O}$ is the distance between the center of the cation and the O atoms of water in the solvation shell, σ is the charge density on the electrode surface in electrons per pm^2, and $r_{H\text{-}el}$ is the distance between the center of the hydrogen atoms in the water molecules of the hydration shell and the electrode surface. For the same cation, the nature of the electrode will only affect σ, which will be determined by the difference between the applied potential and the potential of zero charge (E_{pzc}) and by the interfacial capacitance, C:

$$\sigma = C(E - E_{pzc}) \qquad \text{Eq. 4}$$

Fig. 2 shows the values of the interfacial pH during the electroreduction of CO$_2$ in CO$_2$-saturated M$_2$CO$_3$ solutions at -1 V, as obtained by Singh et al. for Ag and Cu electrodes from their model, and as obtained experimentally by us for an Au electrode. C attains similar values for most metal-electrolyte interfaces, and, although E_{pzc} will be more positive for Au than for Ag and Cu, σ

will be of the same order of magnitude in all three cases.[30] We would expect, hence, similar decreases of the pK_a of a given cation, and similar values of the interfacial pH, for all three cases, if at all, maybe slightly lower in the case of Au. On the contrary, Fig. 2 shows that, although the values of the interfacial pH for Ag and Cu at -1 V estimated by Singh et al. are indeed very similar, they are clearly lower than our experimental values for Au, particularly in the case of the larger cations (K$^+$ and Cs$^+$). This suggests that the decrease of the pK_a at the interface (and consequently, the effect of cation hydrolysis on the interfacial pH) was slightly overestimated by Singh et al.
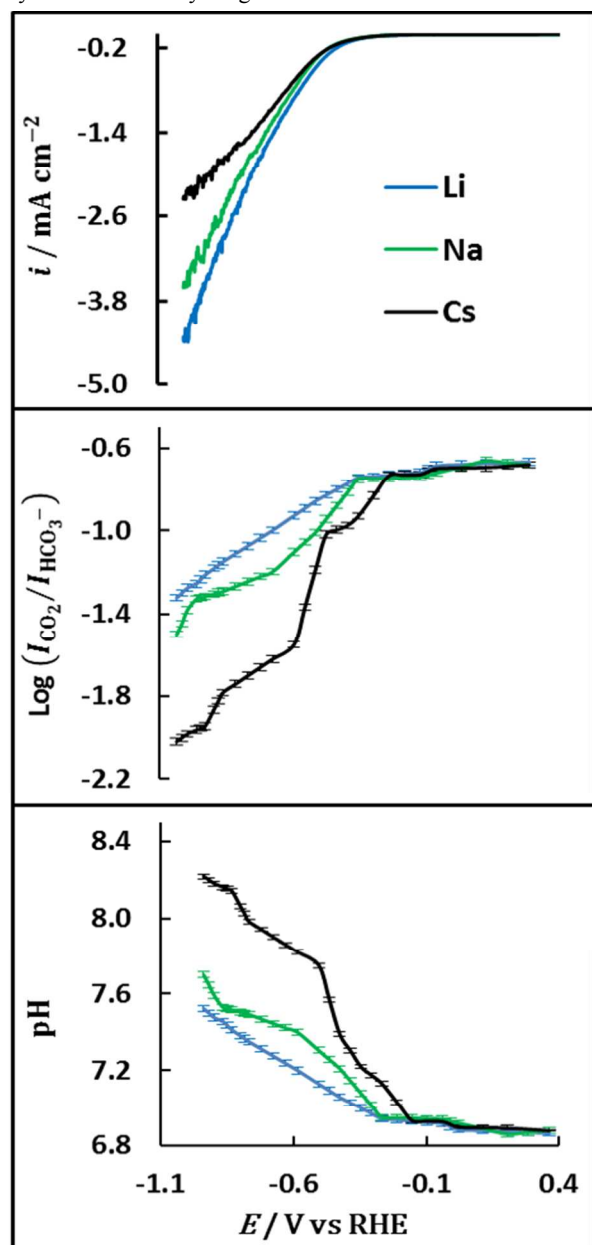

Figure 3. Experiments as in Fig. 1, but using a different set of MHCO$_3$ salts of lower purity to prepare the CO$_2$-bicarbonate buffer solutions.

The reason for the above-mentioned overestimation of the buffering effect of cation hydrolysis in Singh's et al.'s work is an overestimation of σ, mainly due to wrongly calculating it by using the cell voltage (*i.e.*, the difference between the potentials of the working and counter electrodes), instead of $E - E_{pzc}$, and probably also using too high a value for the interfacial capacitance. Too large a value for σ will increase the magnitude of the term accounting for the extra polarization of the solvation water molecules at the interface (see Eq. 3), an effect which will be larger the larger the cation (*i.e.*, r_{M-O}), as indeed observed when comparing our experimental results with their simulations. The effect of overestimating σ might be compensated in part by an overestimation of r_{H-el}, as Singh et al. assumed Ag and Cu electrodes to be covered by adsorbed CO (CO$_{ad}$). CO is known to adsorb weakly on coinage metals.[31–36] In the absence of CO in the solution, only a small CO coverage is to be expected, as confirmed by the absence of intense CO$_{ad}$ bands in our spectra. In any case, our results provide strong experimental support to the cation-dependent buffering effect proposed by Singh et al., although we believe that their simulations can be improved with more realistic values of σ and r_{H-el}.

We would also like to comment on the importance of the purity of the salts employed to prepare the electrolyte solutions. We performed additional series of experiments using CO$_2$-bicarbonate buffer solutions prepared with M$_2$CO$_3$ and MHCO$_3$ salts that we gathered from the labs and stores in our Department, of lower purity. These experiments, shown in Fig. 3, yielded a trend exactly opposite to that shown in Fig. 1, *i.e.*, the current density in a negative-going LSV increases in the series Cs$^+$ < Na$^+$ < Li$^+$. However, it still holds that the cation for which the current is maximum is also the cation for which the increase in the interfacial pH is minimum. This highlights the critical role of the interfacial pH in determining the activity (and, most likely, also the Faradaic efficiency) of the CO2RR, in good agreement with recent findings,[37] as well as the importance of using high-purity salts when investigating cation effects. At the optimal pH for the CO2RR, close to 7, any impurity can enhance or counterbalance the decrease of the pK_a of cation hydrolysis of the supporting electrolyte, thereby affecting the actual increase of pH at the electrode-electrolyte interface, and, through it, the activity and faradaic efficiency of the process.

In summary, we have shown that, although during the CO2RR the interfacial pH increases always above that of the bulk solution, the increase is smaller the larger the radius of the electrolyte cation. This is strong experimental support to a recently proposed model,[20] according to which differences in activity and Faradaic efficiency with different alkaline-metal cations are due to a cation-dependent decrease of the pK_a for cation hydrolysis at the interface. We have also shown that, in that work, the decrease in the pK_a of cation hydrolysis was overestimated, particularly for the larger cations, due to an overestimation of the charge density on the electrode surface. Finally, using salts of lower purity to prepare the CO$_2$-bicarbonate buffer solutions, we have shown that the pH is a critical parameter determining the activity and Faradaic efficiency of the CO2RR, and that extreme care must be taken when selecting the chemicals to investigate the role of cations in the CO2RR, as the presence of impurities can even invert the observed trends.

ASSOCIATED CONTENT

Supporting Information

The Supporting Information is available free of charge on the ACS Publications website.

Experimental details. Figures S1-S4.

AUTHOR INFORMATION

Corresponding Author

e-mail address: angel.cuestaciscar@abdn.ac.uk

REFERENCES

(1) Hori, Y. Electrochemical CO2 Reduction on Metal Electrodes. In *Modern Aspects of Electrochemistry*; Vayenas, C. G., White, R. E., Gamboa-Aldeco, M. E., Eds.; Springer: New York, 2008; Vol. 42, pp 89–189.

(2) Hori, Y.; Wakebe, H.; Tsukamoto, T.; Koga, O. Electrocatalytic Process of CO Selectivity in Electrochemical Reduction of CO_2 at Metal Electrodes in Aqueous Media. *Electrochim. Acta* **1994**, *39*, 1833–1839.

(3) Hori, Y.; Takahashi, I.; Koga, O.; Hoshi, N. Selective Formation of C2 Compounds from Electrochemical Reduction of CO_2 at a Series of Copper Single Crystal Electrodes. *J. Phys. Chem. B* **2002**, *106*, 15–17.

(4) Rodes, A.; Pastor, E.; Iwasita, T. Structural Effects on CO_2 Reduction at Pt Single-Crystal Electrodes: Part 3. Pt(100) and Related Surfaces. *J. Electroanal. Chem.* **1994**, *377*, 215–225.

(5) Hoshi, N.; Ito, H.; Suzuki, T.; Hori, Y. CO2 Reduction on Rh Single Crystal Electrodes and the Structural Effect. *J. Electroanal. Chem.* **1995**, *395*, 309–312.

(6) Hoshi, N.; Suzuki, T.; Hori, Y. Step Density Dependence of CO_2 Reduction Rate on Pt(S)-[n(111) × (111)] Single Crystal Electrodes. *Electrochim. Acta* **1996**, *41*, 1647–1653.

(7) Tang, W.; Peterson, A. A.; Varela, A. S.; Jovanov, Z. P.; Bech, L.; Durand, W. J.; Dahl, S.; Norskov, J. K.; Chorkendorff, I. The Importance of Surface Morphology in Controlling the Selectivity of Polycrystalline Copper for CO_2 Electroreduction. *Phys. Chem. Chem. Phys.* **2012**, *14*, 76–81.

(8) Kim, Y.-G.; Baricuatro, J. H.; Javier, A.; Gregoire, J. M.; Soriaga, M. P. The Evolution of the Polycrystalline Copper Surface, First to Cu(111) and Then to Cu(100), at a Fixed CO2RR Potential: A Study by Operando EC-STM. *Langmuir* **2014**, *30*, 15053–15056.

(9) Hori, Y.; Kikuchi, K.; Murata, A.; Suzuki, S. Production of methane and ethylene in electrochemical reduction of carbon dioxide at copper electrode in aqueous hydrogencarbonate solution. *Chem. Lett.* **1986**, *15*, 897–898.

(10) Paik, W.; Andersen, T. N.; Eyring, H. Kinetic Studies of the Electrolytic Reduction of Carbon Dioxide on the Mercury Electrode. *Electrochim. Acta* **1969**, *14*, 1217–1232.

(11) Hatsukade, T.; Kuhl, K. P.; Cave, E. R.; Abram, D. N.; Jaramillo, T. F. SI Insights into the Electrocatalytic Reduction of CO_2 on Metallic Silver Surfaces. *Phys. Chem. Chem. Phys.* **2014**, *16*, 13814–13819.

(12) Murata, A.; Hori, Y. Product Selectivity Affected by Cationic Species in Electrochemical Reduction of CO_2 and CO at a Cu Electrode. *Bull. Chem. Soc. Jpn.* **1991**, *64*, 123–127.

(13) Frumkin, A. N. Wasserstoffuberspannung Und Struktur Der Doppelschicht. *Z. Phys. Chem.* **1933**, *164*, 121.

(14) Strmcnik, D.; Kodama, K.; van der Vliet, D.; Greeley, J.; Stamenkovic, V. R.; Marković, N. M. The Role of Non-Covalent Interactions in Electrocatalytic Fuel-Cell Reactions on Platinum. *Nat. Chem.* **2009**, *1*, 466–472.

(15) Frumkin, A. N. Influence of Cation Adsorption on the Kinetics of Electrode Processes. *Trans. Faraday Soc.* **1959**, *55*, 156.

(16) Kilic, M. S.; Bazant, M. Z.; Ajdari, A. Steric Effects in the Dynamics of Electrolytes at Large Applied Voltages. I. Double-Layer Charging. *Phys. Rev. E* **2007**, *75*, 21502.

(17) Cabello, G.; Leiva, E. P. M.; Gutierrez, C.; Cuesta, A. Non-Covalent Interactions at Electrochemical Interfaces: One Model Fits All? *Phys. Chem. Chem. Phys.* **2014**, *16*, 14281–14286.

(18) Wildi, C.; Cabello, G.; Zoloff Michoff, M. E.; Vélez, P.; Leiva, E. P. M.; Calvente, J. J.; Andreu, R.; Cuesta, A. Super-Nernstian Shifts of Interfacial Proton-Coupled Electron Transfers: Origin and Effect of Noncovalent Interactions. *J. Phys. Chem. C* **2016**, *120*, 15586–15592.

(19) Escudero-Escribano, M.; Zoloff Michoff, M. E.; Leiva, E. P. M.; Marković, N. M.; Gutiérrez, C.; Cuesta, Á. Quantitative Study of Non-Covalent Interactions at the Electrode–Electrolyte Interface Using Cyanide-Modified Pt(111) Electrodes. *ChemPhysChem* **2011**, *12*, 2230–2234.

(20) Singh, M. R.; Kwon, Y.; Lum, Y.; Ager, J. W.; Bell, A. T. Hydrolysis of Electrolyte Cations Enhances the Electrochemical Reduction of CO_2 over Ag and Cu. *J. Am. Chem. Soc.* **2016**, *138*, 13006–13012.

(21) Osawa, M.; Ikeda, M. Surface-Enhanced Infrared Absorption of P-Nitrobenzoic Acid Deposited on Silver Island Films: Contributions of Electromagnetic and Chemical Mechanisms. *J. Phys. Chem.* **1991**, *95*, 9914–9919.

(22) Luque, A. M.; Cuesta, A.; Calvente, J. J.; Andreu, R. Potentiostatic Infrared Titration of 11-Mercaptoundecanoic Acid Monolayers. *Electrochem. Commun.* **2014**, *45*, 13–16.

(23) Yamakata, A.; Osawa, M. Destruction of the Water Layer on a Hydrophobic Surface Induced by the Forced Approach of Hydrophilic and Hydrophobic Cations. *J. Phys. Chem. Lett.* **2010**, *1*, 1487–1491.

(24) Yamakata, A.; Osawa, M. Destruction of the Hydration Shell around Tetraalkylammonium Ions at the Electrochemical Interface. *J. Am. Chem. Soc.* **2009**, *131*, 6892–6893.

(25) Yamakata, A.; Soeta, E.; Ishiyama, T.; Osawa, M.; Morita, A. Real-Time Observation of the Destruction of Hydration Shells under Electrochemical Force. *J. Am. Chem. Soc.* **2013**, *135*, 15033–15039.

(26) Kyriacou, G. Z.; Anagnostopoulos, A. K. Influence CO_2 Partial Pressure and the Supporting Electrolyte Cation on the Product Distribution in CO_2 Electroreduction. *J. Appl. Electrochem.* **1993**, *23*, 483–486.

(27) Thorson, M. R.; Siil, K. I.; Kenis, P. J. A. Effect of Cations on the Electrochemical Conversion of CO_2 to CO. *J. Electrochem. Soc.* **2012**, *160*, F69–F74.

(28) Baes, C. F.; Mesmer, R. E. *Hydrolysis of Cations*; Wiley Interscience: New York, 1976.

(29) Brown, P.; Ekberg, C. *Hydrolysis of Metal Ions*; Brown, P. L., Ekberg, C., Eds.; Wiley-VCH Verlag GmbH & Co. KGaA: Weinheim, Germany, 2016.

(30) Schmickler, W.; Santos, E. *Interfacial Electrochemistry*, 2nd Ed.; Springer: Berlin / Heidelberg, 2010.

(31) Hori, Y.; Koga, O.; Watanabe, Y.; Matsuo, T. FTIR Measurements of Charge Displacement Adsorption of CO on Poly- and Single Crystal (100) of Cu Electrodes. *Electrochim. Acta* **1998**, *44*, 1389–1395.

(32) Hori, Y.; Wakebe, H.; Tsukamoto, T.; Koga, O. Adsorption of CO Accompanied with Simultaneous Charge Transfer on Copper Single Crystal Electrodes Related with Electrochemical Reduction of CO2 to Hydrocarbons. *Surf. Sci.* **1995**, *335*, 258–263.

(33) Hori, Y.; Koga, O.; Yamazaki, H.; Matsuo, T. Infrared Spectroscopy of Adsorbed CO and Intermediate Species in Electrochemical Reduction of CO_2 to Hydrocarbons on a Cu Electrode. *Electrochim. Acta* **1995**, *40*, 2617–2622.

(34) Hori, Y.; Murata, A. Electrochemical Evidence of Intermediate Formation of Adsorbed CO in Cathodic Reduction of CO_2 at a Nickel Electrode. *Electrochim. Acta* **1990**, *35*, 1777–1780.

(35) Hori, Y.; Murata, A.; Yoshinami, Y. Adsorption of CO, Intermediately Formed in Electrochemical Reduction of CO_2, at a Copper Electrode. *J. Chem. Soc., Faraday Trans.* **1991**, *87*, 125–128.

(36) Cuesta, A.; López, N.; Gutiérrez, C. Electrolyte Electroreflectance Study of Carbon Monoxide Adsorption on Polycrystalline Silver and Gold Electrodes. *Electrochim. Acta* **2003**, *48*, 2949–2956.

(37) Birdja, Y. Y.; Koper, M. T. M. The Importance of Cannizzaro-Type Reactions during Electrocatalytic Reduction of Carbon Dioxide. *J. Am. Chem. Soc.* **2017**, *139*, 2030–2034.

$$pH \propto -\log \frac{I_{CO_2}}{I_{HCO_3^-}}$$